Pure & Appl. Chem., Vol. 70, No. 3, pp. 555–565, 1998.
Printed in Great Britain.

Structure-based inhibitor design for CDK2, a cell cycle controlling protein kinase

Sung-Hou Kim, Department of Chemistry and E. O. Lawrence Berkeley National Laboratory, University of California, Berkeley, California 94720 U.S.A.

Abstract: The central role of cyclin-dependent kinases (CDKs) in cell cycle regulation makes them a promising target for discovering small inhibitory molecules that can modify the degree of cell proliferation. The three-dimensional structure of CDK2 provides a structural foundation for understanding the mechanisms of activation and inhibition of CDK2 and for the discovery of the inhibitors. In this presentation five structures of human CDK2 are summarized: apo protein, ATP complex, olomoucine complex, isopentenyladenine complex, and flavopiridol complex. This structural information is used for the design of a small, directed combinatorial library.

INTRODUCTION

Cell cycle progression is tightly controlled by the activity of cyclin-dependent kinases (CDKs) (refs. 1-3). CDKs remain inactive by themselves, and activation requires binding to cyclins, a diverse family of proteins whose levels oscillate during the cell cycle, and phosphorylation by CDK-activating kinase (CAK) on a specific threonine residue (refs. 4, 5). In addition to the positive regulatory proteins such as cyclins and CAK, many negative regulatory proteins (CDK inhibitory proteins, CKIs) have been discovered (refs. 6-8) such as p16 (ref. 9), p21 (refs. 10-13), and p28 (ref. 14). Since deregulation of cyclins and/or alteration or absence of CKIs have been associated with many cancers, there is strong interest in chemical inhibitors of CDKs that could play an important role in the discovery of a new family of anti-tumor agents or anti-proliferative drugs.

Since ATP is the authentic cofactor of CDK2 it can be considered as a "pseudo-lead compound" for discovery of CDK2 inhibitors. However there are two major concerns: adenine-containing compounds are common ligands for many enzymes in cells, thus, any adenine derivatives may inhibit many enzymes in the cells: second, any compounds with highly charged groups such as phosphates in ATP will prevent uptake by the cells. Our studies provide the structural basis for overcoming the two difficulties by appropriate modification of a common base such as adenine to endow specificity and cell uptake of the derivatives. The results summarized here are obtained in collaboration with the laboratories of David Morgan at the University of California, San Francisco, Peter Schultz at the University of California, Berkeley, Laurent Meijer of CNRS-Roscoff in France, and Peter Worland and Edward Sausville of NIH.

MATERIALS AND METHODS

Materials

Human CDK2 was prepared as described in Ref. 15. Briefly, Sf9 insect cells were infected with baculovirus containing a human CDK2 gene. The supernatant of cell lysate was loaded over a DEAE Sepharose column followed by an S-Sepharose column. The flow-through was loaded onto an ATP-affinity column and eluted by NaCl salt gradient. The purified protein is fully functional in that it binds to cyclin A, the resulting complex can be fully activated when incubated with partially purified human CAK, and phosphorylated CDK2-cyclin A complex can phosphorylate histon H1.

Olomoucine was obtained from L. Meijer of CNRS, Roscoff, France, and isopentenyladenine and ATP were purchased from Sigma (St. Louis, Missouri). Des-chloro-flavopiridol and flavopiridol are derived by chemical synthesis from a parent structure obtained from Dysoxylum binectariferum (ref. 16), a plant native to India. Both were provided by Dr. Peter Worland now at Mitotix (Cambridge, Massachusetts) who obtained it from Dr. Harald Sedlacek, Behringwerke, Marburg, Germany. The chemical structures of ATP and the inhibitors discussed are shown in Fig. 1.

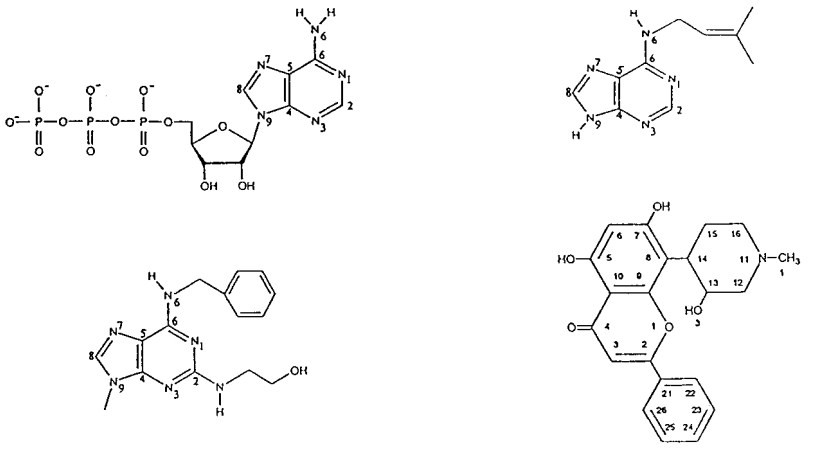

Fig. 1. Chemical structures of four ligands of CDK2 discussed in this paper: (top left) ATP, (bottom left) olomoucine, (top right) isopentenyladenine, and (bottom right) des-chloro-flavopiridol.

Inhibitor soaking and co-crystals

Recombinant CDK2 was crystallized as below (ref. 17). A CDK2 solution was concentrated to 10 mg/ml by dialysis against 20 mM Hepes buffer (pH 7.4) and 1 mM EDTA. Sitting drops were equilibrated by vapor diffusion at 4°C against reservoirs containing 200 mM Hepes buffer at pH 7.4. Diamond- and wedge-shaped crystals appeared after two to four days. A gradual increase of the Hepes buffer concentration in the reservoirs (up to 800 mM) produced crystals with average dimensions of about 0.2 mm x 0.3 mm x 0.3 mm. After CDK2 crystals had formed, small amounts of powdered chemical inhibitors were added to the crystallization drops. All inhibitor complexes were obtained by this soaking procedure (refs. 18, 19), except for the olomoucine complex, which was obtained by co-crystallization of a precomplexed solution of CDK2 and olomoucine. Crystals were soaked usually for 48 hours before data collection. Crystallization of CDK2 apoprotein and co-crystallization of CDK2 and olomoucine were performed using the sparse matrix method (ref. 20).

X-ray crystallographic studies

Relevant crystallographic parameters and refinement parameters are given in Table 1. X-ray diffraction data were collected using a Rigaku RAXIS-II imaging plate area detector and processed with the RAXIS data processing software. The crystal structure of the apoprotein (ref. 17) was determined by the multiple isomorphous replacement method, and ATP complex structure as well as all the inhibitor complex structures (refs. 17, 18, 19) were solved by the molecular replacement method using the apo structure as the probe. All the structures were refined using X-PLOR 3.0 (ref. 22). The refinement statistics are given also in Table 1.

RESULTS

Domain structure and conformation of CDK2

The CDK2 structure is almost identical in CDK-apoenzyme (ref. 17), ATP complex (ref. 17), olomoucine complex (ref. 18), isopentenyladenine complex (ref. 18), des-chloro-flavopiridol (ref. 19), and flavopiridol complex (unpublished), and very similar to that in CDK2-cyclin A complex (ref. 23), except in five regions (see below). The enzyme is folded into the bilobal structure typical for most of protein kinases, with the smaller N-terminal domain consisting predominantly of β-sheet structure and the larger C-terminal domain consisting primarily of α-helices (Fig. 2). There are no significant differences in the domain orientations between the ligand-enzyme complexes and the apoenzyme. In all cases except CDK2-cyclin A complex (ref. 23), electron density is weak in two regions in the enzyme, spanning residues 36-47 which links the N-terminal

TABLE 1. Crystallographic parameters and refinement statistics.

	APO	ATP	Olomoucine	Isopentenyladenine	Des-chloroflavopiridol
Space group	$P2_12_12_1$	$P2_12_12_1$	$P2_12_12_1$	$P2_12_12_1$	$P2_12_12_1$
Cell dimensions (Å)	a=73.12	a=72.82	a=73.77	a=73.25	a=71.30
	b=72.72	b=72.66	b=72.55	b=72.51	b=72.03
	c=54.25	c=54.07	c=54.06	c=54.03	c=53.70
Unique reflections	27,034	22,636 (3,019)	15,044	25,371	11,430
Completeness of data (Å)	∞—1.8 98.6%	∞—1.9	∞—2.5 99.0%	∞—2.0 96.4%	∞—2.0 91.7%
	1.9—1.8 97.1%		2.5—2.2 97.0%	2.0—1.8 84.0%	
R_{sym}* (%)	6.1	6.7	8.4	8.3	4.9
Resolution (Å)	8.00—1.8	8.00—1.8	8.00—2.2	8.00—1.8	8.00—2.33
R_{value}*	0.18	0.18	0.19	0.20	20.3
R_{free} †	0.25	0.27	0.27	0.27	28.8
$B_{average}$#(Å^2)	31	38	31	30	32.35
Deviations observed:					
rmsd from ideal bond length (Å)	0.011	0.012	0.013	0.011	0.012
rmsd from ideal bond angle (°)	1.61	1.78	1.70	1.76	1.7
Number of water molecules	180	108	76	99	84

*R_{value}= $100\Sigma|F_O - F_C|/\Sigma(F_O)$, the sums being taken over all reflections with F/s(F) > 2 cutoff.

†R_{free} = R_{value} for 10% of the data, which were not included during crystallographic refinement.

#$B_{average}$ = Average *B values* for all non-hydrogen atoms.

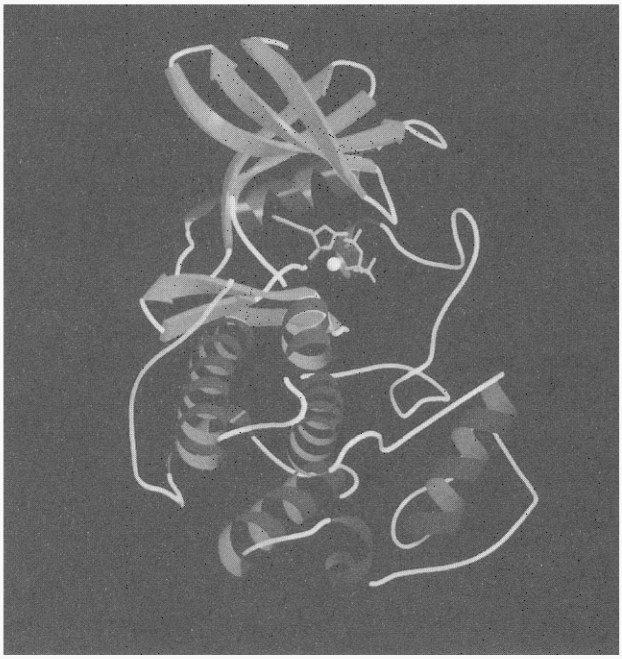

Fig. 2. The backbone structure of human CDK2. The β-strands and α-helices are represented by green arrowed ribbons and helical coils, respectively, and ATP in a yellow stick model and Mg++ ion as a white ball. All the connectors between secondary structures are shown as yellow coils.

domain and "PSTAIR" or cyclin recognition helix and residues 150-164 of the "T-loop" containing the activating phosphorylation site. All inhibitors and ATP bind in the deep cleft between the two domains. Most of the conserved residues among CDKs are located either around the ATP-binding pocket or ATP-binding side of CDK2.

Conformational differences between active and inactive form of CDK2 and a mechanism of activation

Comparison of the structure of CDK2 in ATP complex (ref. 17) and the ternary complex of CDK2 with ATP and cyclin (ref. 21) shows that there are five significant conformational differences: (1) the two domains are more open in the ternary complex, thus, pushing the phosphate-loop (P-loop) toward the N-terminal domain; (2) the conformation of the triphosphate of ATP and surrounding residues are different; (3) on cyclin A binding, the short α-helix becomes a β-strand in the α/β transition box; (4) the "T-loop" containing Thr160, which gets phosphorylated for CDK2 to be fully activated, reorients completely; and (5) "PSTAIR or cyclin-binding helix" changes its location and orientation. These differences are schematically shown in Fig. 3. The conformational changes of the residues surrounding ATP, which in turn changes the conformation of the triphosphate of ATP so that the scissile bond between β- and γ-phosphates now becomes "in line" to the direction of attacking hydroxyl oxygen of the substrates of CDK2, the necessary alignment for ATP hydrolysis.

Interaction between CDK2 and ligands

(A) ATP

The binding site for ATP as well as the inhibitors is located between the N- and C-terminal domains (Fig. 4), and the binding of these ligands are associated with conformational changes of surrounding residues. The refinement of the CDK2 apoenzyme and ATP complex to 1.8 Å and 1.9 Å, respectively, resulted in very accurate protein models as indicated by low R-values and good stereochemistry. The electron density for the refined CDK2-ATP complex shows clear density for the ATP molecule with all three phosphates, a Mg2+ ion, and a few water molecules in the binding pocket. The five-membered ribose ring is puckered into a C2'-endo envelope (ref. 17).

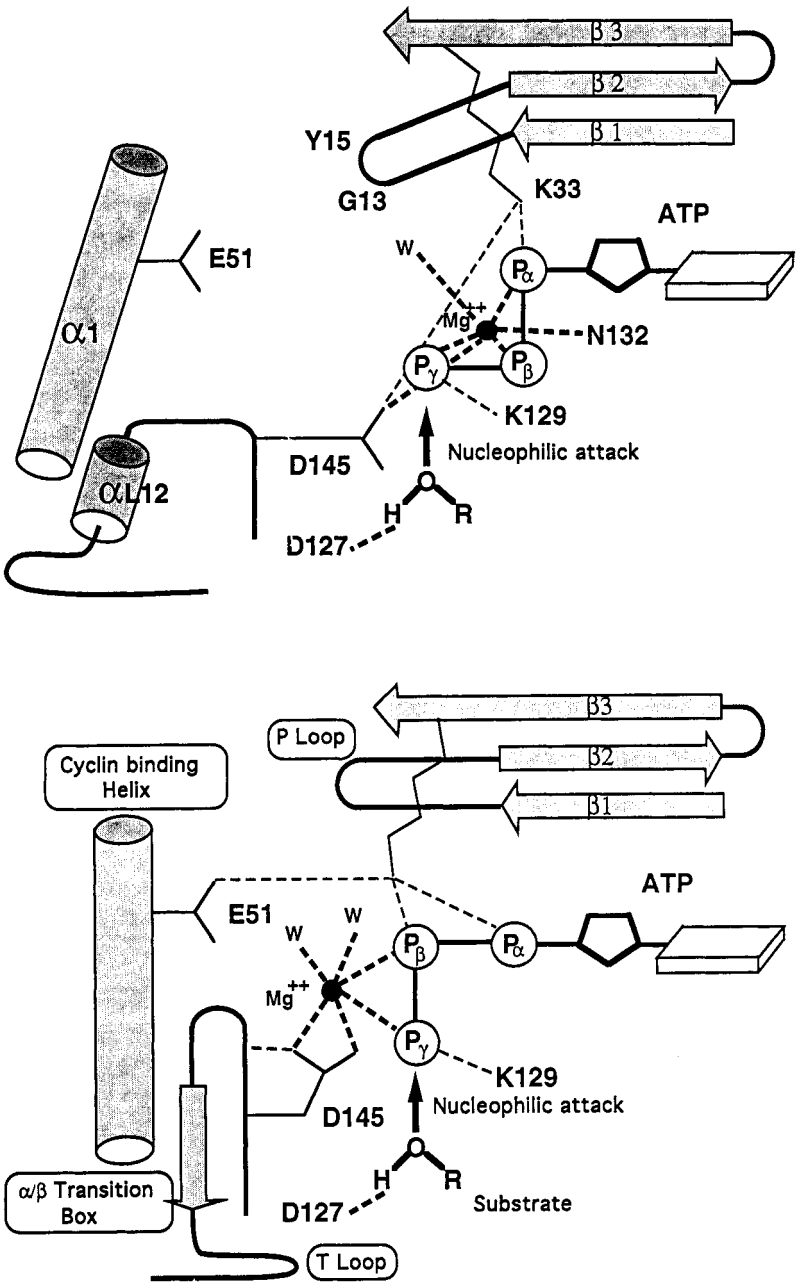

Fig. 3. Schematic drawing of the five regions that have different conformations between (a) CDK-ATP binary complex, and (b) CDK2-ATP-cyclin A ternary complex structures. They are: triphosphate of ATP, P-loop, cyclin-binding helix, α/β transition box, and T-loop.

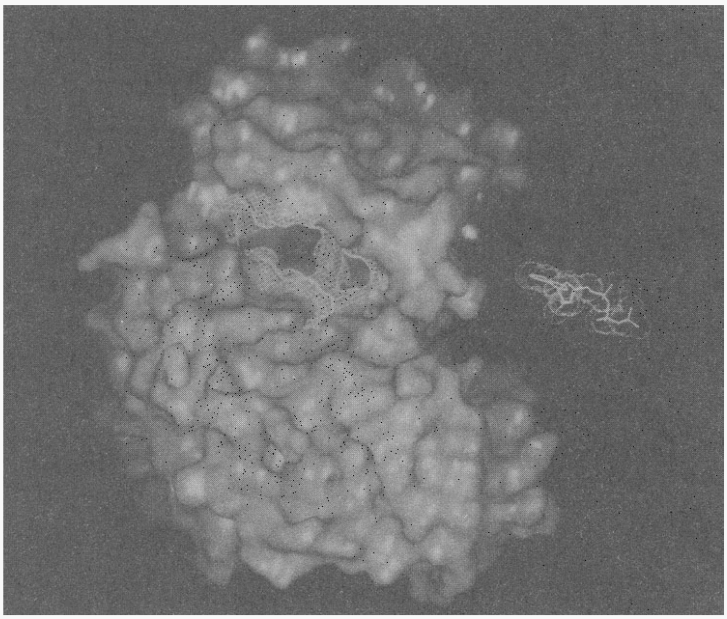

Fig. 4. Molecular surface of CDK2 and ATP-binding pocket. ATP was moved out of the pocket for clarity.

As can be expected from the relative hydrophilicity of the ATP molecule, most hydrogen bonds and salt bridges are formed with the phosphate moieties, while the adenine base and ribose areinvolved in only three hydrogen bonds each (Fig 5). Three water molecules in the binding pocket are also mediating CDK2-ATP interactions. The hexacoordinated Mg2+ ion is bound by one oxygen from each phosphate, and one from Asn132 and Asp145 side-chains and one water.

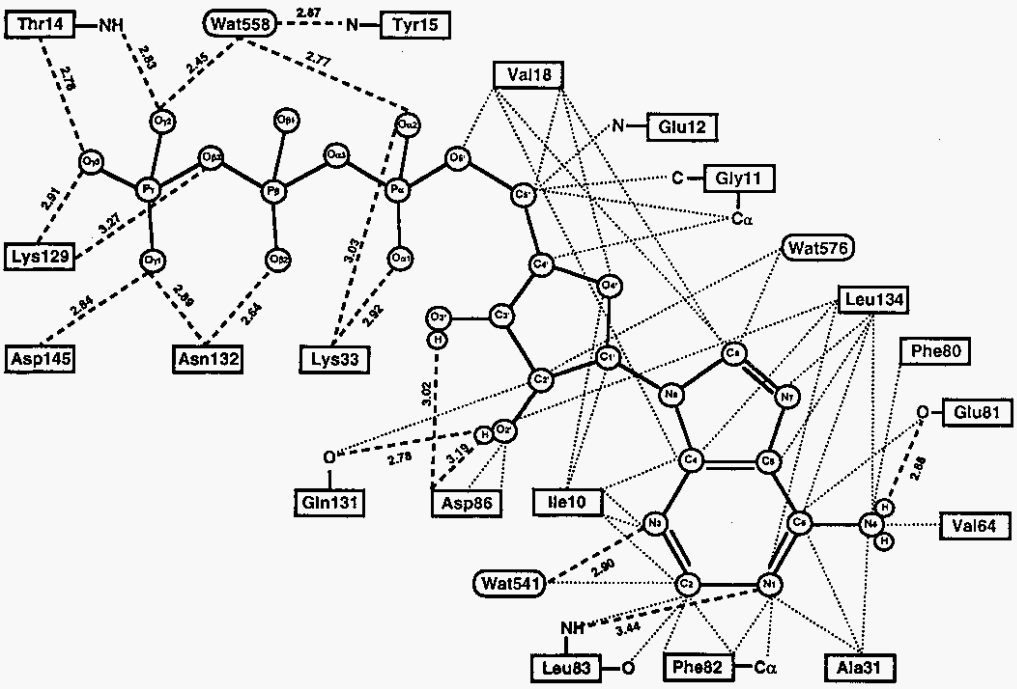

Fig. 5. All atomic interactions between CDK2 and ATP. Contacts with protein side-chains are indicated by lines connecting to the respective residue box while interactions to main-chain atoms are shown as lines to the specific main-chain atoms indicated. Van der Waals contacts are indicated by dotted lines, and hydrogen bonds by thick broken lines. For ATP van der Waals contacts to phosphates were omitted for clarity.

(B) Adenine derivative inhibitors: olomoucine and isopentenyladenine

Kinase assay of adenine derivatives revealed that two adenine derivatives have inhibitory properties of CDC2 and CDK2 with IC_{50} of about 10 mM range: olomoucine inhibits cell cycle kinases (except CDK4) quite specifically, and isopentenyladenine (IPA) inhibits both cell cycle kinases and non-cell cycle kinases.(ref. 23). The crystal structures of CDK2-IPA complex and CDK2-olomoucine complex have been determined to high resolution (1.8 Å and 2.2 Å respectively), with good stereochemistry (Table 1). As in the apoenzyme and in the CDK2-ATP complex, electron density is weak for two regions in the enzyme spanning residues 37-43 of interdomain connector and 153-163 of the T-loop containing the activating Thr160 phosphorylation site (ref. 17).

Both IPA and olomoucine are adenine derivatives. Although the purine rings bind roughly in the same area of the binding cleft as the adenine ring of ATP, the relative orientation of each purine ring with respect to the protein is different for all three ligands (ATP, IPA, and olomoucin) as shown in Fig. 6. This is probably due to the different size of the substituent groups of the purine

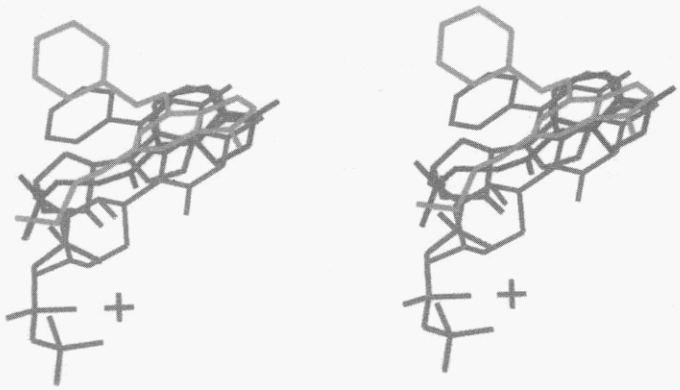

Fig. 6. A stereo view of the superposition of ATP (red), olomoucin (green), des-chloro-flavopiridol (purple), and isopentenyladenine (blue) in the ATP-binding pocket of CDK2

in the three ligands; the N6 amino group of the adenine ring is replaced by an isopentenylamino group in IPA and by a bulky benzylamino group in olomoucine. The complete atomic interaction between CDK2 and olomoucine is shown in Fig. 7, and that between CDK2 and IPA in Fig. 8.

(C) A flavone inhibitor: des-chloro-flavopiridol

Previous studies have shown that flavopiridol, a novel flavonoid which is not an adenine derivative, can inhibit growth of breast and lung carcinoma cell lines and can inhibit CDK activity at the same nanomolar concentration range of the inhibitor (ref. 16). To understand how flavopiridol analogs bind to the ATP pocket, we determined the X-ray structure of CDK2 in complex with the flavopiridol and des-chloro-flavopiridol (DFP, Fig. 1), and compared it with the X-ray structures of CDK2-ATP complex (ref. 17) and other inhibitor complexes of CDK2 (ref. 18). Flavopyridol binds to CDK2 in the same manner as DFP.

DFP binds in the ATP-binding pocket, with the benzopyran ring occupying approximately the same region as the purine ring of ATP (Fig. 6). The two ring systems overlap in the same plane, but the benzopyran is rotated about 60° relative to the adenine in ATP, measured as the angle between the carbon-carbon bonds joining the two cycles in benzopyran and adenine rings, respectively. In this orientation, the O5 hydroxyl and the O4 of the inhibitor are close to the position of the N6 amino group and N1 in adenine, respectively. The piperidinyl ring partially occupies the α-phosphate pocket and is assigned to a chair conformation (although a boat conformation can not be ruled out in the current resolution map). The detail interactions between DFP and CDK2 are shown in Fig. 9.

Differences in protein side-chain conformations in the binding pocket

In contrast to the finding that cyclin A changes very little on CDK2 binding (ref. 21), the conformation of CDK2 appears to be much more adaptable as manifested by its changes on binding of ATP, olomoucin, IPA and DFP, as well as cyclin A (refs. 17, 18, 19, 21). To find out whether any inhibitor or ATP binding to CDK2 induces changes in side-chain conformation in the

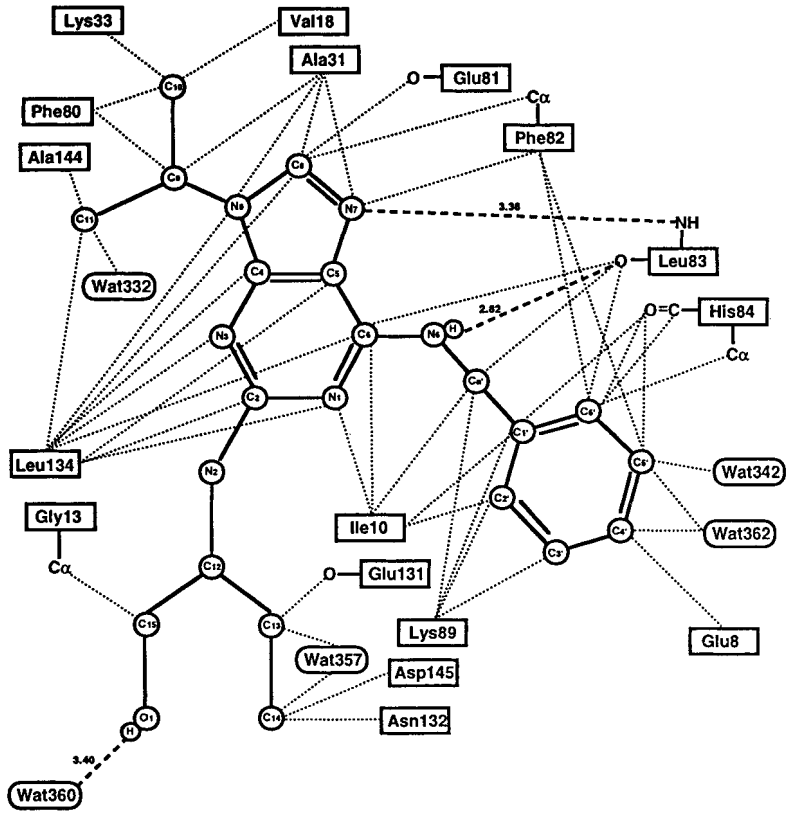

Fig. 7. All atomic interactions between CDK2 and olomoucine. The rest of the legend is the same as that of Fig. 5. All ligand contacts are shown.

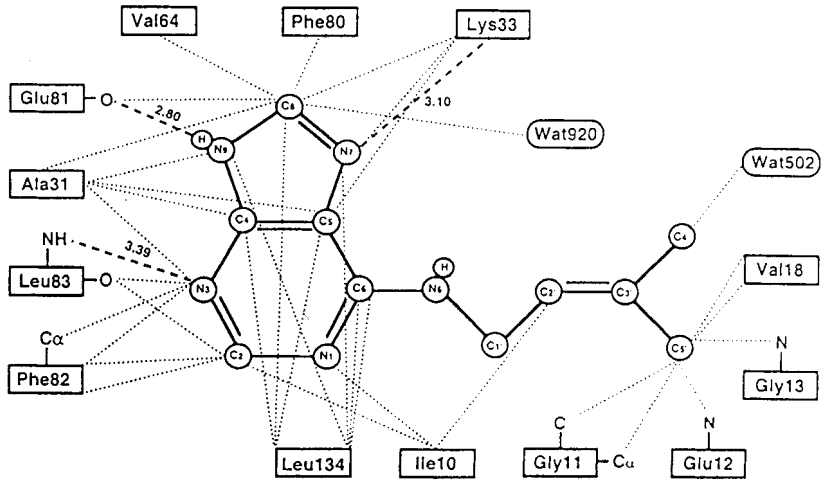

Fig. 8. All atomic interactions between CDK2 and isopentenyladenine. The rest of the legend is the same as that of Fig. 5. All ligand contacts are shown.

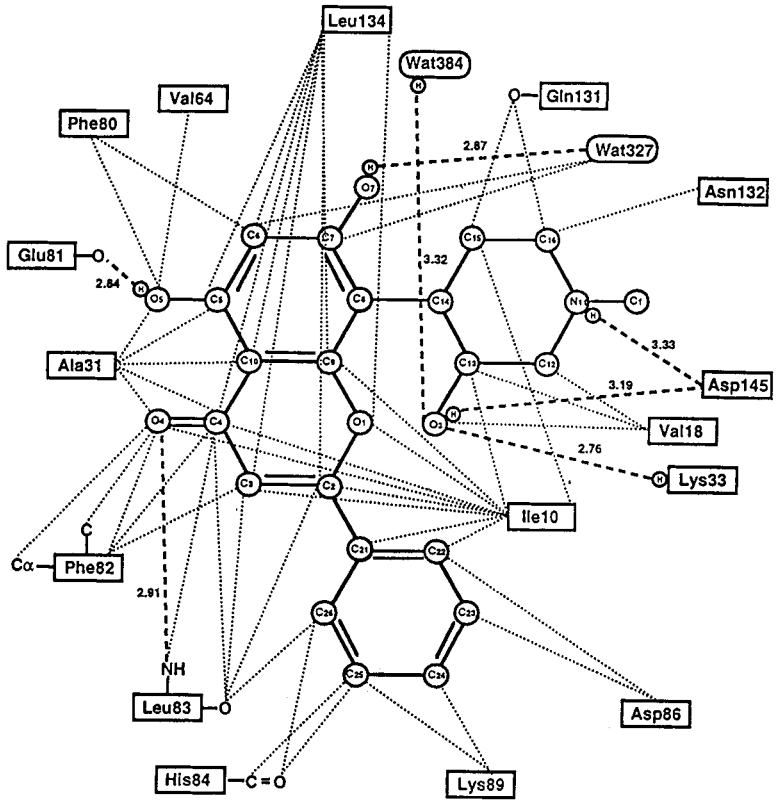

Fig. 9. All atomic interactions between CDK2 and des-chloro-flavopiridol. The rest of the legend is the same as that of Fig. 5. All ligand contacts are shown.

binding pocket, we compared the binding pockets of CDK2-ligand complexes and CDK2 apo protein after a superposition of the enzymes based on their Cα atoms. This superposition revealed the significant movement of few side-chains. In addition to the P-loop, four residues change their side chain conformations most: Lys33, Q131, Ile10, and N132. Lys33 and its equivalent Lys72 in cyclic AMP dependent protein kinase are important for ATP binding. In all ligand bound complexes the side chain of this residue has moved away to accommodate the ligands except IPA complex, where the side chain conformation is the same as that of apoenzyme presumably because of the small size of the ligand. In the CDK2-ATP complex, Lys33 forms salt bridges with the a phosphate of ATP and Asp145, another residue involved in ATP-Mg2+ binding (ref. 17).

The side-chain of Gln131 is directed away from the binding pocket in the ATP and IPA complex. In the olomoucine complex, however, the side-chain points into the binding pocket and forms van der Waals contacts and a hydrogen bond with the hydroxyethylamino group of olomoucine. Ile10 and Asn132 make smaller conformational changes on the ligand binding. In summary, the observed side-chain differences in the binding pocket seem to contribute to an improved fit between protein and ligand molecules.

Structure-based combinatorial library

Using the crystal structure of the complex between CDK2 and olomoucine we have chosen three sites of adenine for introducing various chemical groups in our combinatorial libraries. Peter Schultz's laboratory at University of California-Berkeley synthesized three classes of small combinatorial libraries using three different sites of adenine to conjugate to the solid plastic pins in 8 x 12 arrays (ref. 26). *In vitro* assay for the inhibition of CDK2 activities were measured using histone H1 as a substrate. Compared to olomoucine, which has IC50 of about 10 μM under our assay condition, the best inhibitors identified from the three libraries have about three orders of magnitude greater potency (IC 50 of about 15 nM) than olomoucine (manuscript in preparation).

DISCUSSION

The high-resolution X-ray structures of human CDK2 apoenzyme and ATP complex as well as CDK2-cyclin A-ATP complex provide the structural basis for understanding the mechanism of activation of CDK2. Furthermore, the structures of the complexes between CDK2 with four inhibitors described here explain the specificity and potency of these inhibitors compared to other related derivatives, and suggest structure-based drug design and combinatorial library design that may enhance the chance of discovering better and improved inhibitors of CDK2 and other CDKs. Several interesting lessons were learned from these structural studies:

(a) The ATP-binding pocket of CDK2 has the surprising capacity to bind varieties of flat aromatic moieties with some unpredictable conformational changes of residues in the pocket. This may be related to the relatively weak binding of the ligands (Kd ~μM).

(b) Knowing the orientation of adenine of ATP in the ATP pocket did not allow us to predict how the adenine moiety of olomoucine and IPA would bind to CDK2. Experimental determination of IPA and olomoucine complexes made us realize that any "rational drug design" based on adenine position of ATP would have completely missed in predicting olomoucine and IPA as potential inhibitors.

(c) Specificity of each inhibitor for CDK2 over other kinase comes from the interaction between substitution groups outside of the aromatic scaffold and the peripheral surface of the ATP pocket. This observation dispels the conventional wisdom that "the common base such as adenine cannot be a good scaffold for inhibitor design because there are many proteins in cells that bind adenine derivatives." Our results clearly demonstrate that specificity can be created by appropriate modification of a common scaffold molecule.

(d) The knowledge of the structures of CDK2 complexes with the three inhibitors suggests a few new scaffolds to consider in structure-based drug design and combinatorial library design.

(e) Structure-based design of combinatorial library is a highly effective way of discovering improved inhibitors (refs. 24, 25).

(f) Structure-based combinatorial library design is an effective way to improve the potency of an inhibitor.

REFERENCES

1. C. Norbury and P. Nurse. *Annu. Rev. Biochem.* **61**, 441–470 (1992).
2. F. Fang and J. W. Newport. *Cell* **66**, 731–742 (1991).
3. T. Hunt. *Curr. Opin. Cell Biol.* **1**, 274–286 (1989).
4. D. Desai, Y. Gu and D. O. Morgan. *Mol. Biol. Cell* **3**, 571–582 (1992).
5. Y. Gu, J. Rosenblatt and D. O. Morgan. *EMBO J.* **11**, 3995–4005 (1992).
6. H. E. Richardson, C. S. Stueland, J. Thomas, P. Russel and S. I. Reed. *Genes Dev.* **4**, 1332–1344 (1990).
7. M. Serrano, G. J. Hannon and D. Beach. *Nature* **366**, 704–707 (1993).
8. M. Peter and I. Herskowitz. *Cell* **79**, 181–184 (1994).
9. T. Nobori, K. Miura, D. J. Wu, A. Lois, K. Takabayashi and D. A. Carson. *Nature* **368**, 753–756 (1994).
10. Y. Gu, C. W. Turck and D. O. Morgan. *Nature* **366**, 707–710 (1993).
11. Y. Xiong, G. J. Hannon, H. Zhang, D. Casso, R. Kobayashi and D. Beach. *Nature* **366**, 701–704 (1993).
12. J. W. Harper, G. R. Adami, N. Wei, K. Keyomarsi and S. J. Elledge. *Cell* **75**, 805–816 (1993).
13. V. Dulic, W. K. Kaufmann, S. J. Wilson, T. D. Tisty, E. Lees, J. W. Harper and S. J. Elledge. *Cell* **76**, 1013–1023 (1994).
14. L. Hengst, V. Dulic, J. M. Slingerland, E. Lees and S. I. Reed. *Proc. Natl. Acad. Sci., USA* **91**, 5291–5295 (1994).
15. H. L. De Bondt, J. Rosenblatt, J. Jancarik, H. D. Jones, D. O. Morgan and S.-H. Kim. *Nature* **363**, 595 (1993).
16. M. D. Losiewicz, A. C. Bradley, G. Kaur, E. A. Sausville and P. J. Worland. *Biochem. Biophys. Res. Commun.* **201**, 589–595 (1994); G. Kaur, M. Stetler-Stevenson, S. Seber, P. Wordland, H. Sedlacek, C. Myers, J. Czech, R. Naik and E. Sausville. *J. Natl. Cancer Inst.* **84**, 1736–1740 (1992).
17. H. L. De Bondt, J. Rosenblatt, J. Jancarik, H. D. Jones, D. O. Morgan and S.-H. Kim. *Nature* **363**, 595–602 (1993).
18. U. Schulze-Gahmen, J. Brandsen, H. D. Jones, D. O. Morgan, L. Meijer, J. Vesely and S.-H. Kim. *Proteins: Structure, Function, and Genetics* **22**, 378–391 (1995).
19. W. F. Azevedo Jr., H.-J. Müeller-Dieckmann, U. Schulze-Gahmen, P. J. Worland, E. Sausville and S.-H. Kim. In press, *Proc. Natl. Acad. Sci.*, USA, (1996).

20. J. Jancarik and S.-H. Kim. *J. Appl. Cryst.* **24**, 409–411 (1991).
21. P. D. Jeffrey, A. A. Russo, K. Polyak, E. Gibbs, J. Hurwitz, J. Massagué and N. P. Pavletich. *Nature* **376**, 313–320 (1995).
22. A. T. Brünger. *X-PLOR, a System for Crystallography and NMR, Version 3.0.* Yale University Press, New Haven, CT (1991).
23. J. Vesely, L. Havlicek, M. Strand, J. J. Blow, A. Donella-Deana, L. Pinna, D. S. Letham, J.-Y. Kato, L. Detrivaud, S. Leclerc and L. Meijer. *Eur. J. Biochem.* **224**, 771–786 (1994).
24. T. C. Norman, N. S. Gray, J. T. Koh and P. G. Schultz. *J. Am. Chem. Soc.* **118**, 7430–7431 (1996).
25. N. S. Gray, S. Kwon and P. G. Schultz. *Tet. Letter* **38**, 1161–1164 (1997).
26. H.M. Geyson, R.H. Meloen, and S.J. Barteling. *Proc. Natl. Acad. Sci. U.S.A.* **81**, 3998-4002 (1984).